sustainability

MDPI

Article

Research on Public Air Route Network Planning of Urban Low-Altitude Logistics Unmanned Aerial Vehicles

Honghai Zhang, Tian Tian, Ouge Feng, Shixin Wu and Gang Zhong *

College of Civil Aviation, Nanjing University of Aeronautics and Astronautics, Nanjing 211106, China
* Correspondence: zg1991@nuaa.edu.cn

Abstract: As urban populations continue to grow and road traffic congestion worsens, traditional ground logistics has become less efficient. This has led to longer logistics times and increased costs. Therefore, unmanned aerial vehicle (UAV) logistics has become increasingly popular. However, free-planned routes cannot meet the safety and efficiency requirements of urban airspace mobility. To address this issue, a public air route network for low-altitude logistics UAVs needs to be established in urban areas. This paper proposes a public route network planning method based on the obstacle-based Voronoi diagram and A* algorithm, as follows: Firstly, construct a city airspace grid model in which the characteristics of the airspace are mapped onto the grid map. Introduce an obstacle clustering algorithm based on DBSCAN to generate representative obstacle points as the Voronoi seed nodes. Utilize the Voronoi diagram to establish the initial route network. Then, conduct an improved path planning by employing the A* algorithm for obstacle avoidance in route edges that pass through obstacles. To ensure the safe operation of drones, set constraints on the route safety interval. This process will generate a low-altitude public air route network for urban areas. After considering the flight costs of logistics UAVs at different altitudes, the height for the route network layout is determined. Finally, the route network evaluation indicators are established. The simulation results demonstrate that compared with the city road network planning method and the central radial network planning method, the total route length is shortened by 7.1% and 9%, respectively, the airspace coverage is increased by 9.8% and 35%, respectively, the average network degree is reduced by 52.6% and 212%, respectively, and the average flight time is reduced by 19.4s and 3.7s, respectively. In addition, by solving the network model using the Dijkstra algorithm, when the energy cost and risk cost weights are 0.6 and 0.4, respectively, and the safety interval is taken as 15 m, the total path cost value of the planned trajectory is minimized.

Keywords: logistics unmanned aerial vehicle; urban air mobility; Voronoi diagram; A* algorithm; public air route network

Citation: Zhang, H.; Tian, T.; Feng, O.; Wu, S.; Zhong, G. Research on Public Air Route Network Planning of Urban Low-Altitude Logistics Unmanned Aerial Vehicles. *Sustainability* **2023**, *15*, 12021. https://doi.org/10.3390/su151512021

Academic Editor: Maxim A. Dulebenets

Received: 6 July 2023
Revised: 31 July 2023
Accepted: 31 July 2023
Published: 5 August 2023

1. Introduction

With the rapid development of artificial intelligence and the advent of the Internet era, UAV logistics has gradually entered the public's field of vision as an emerging technology with tremendous potential [1]. Particularly in the field of logistics, UAV logistics is considered a promising and widely applicable new transportation mode that can effectively address the "last-mile" delivery challenges [2]. At the same time, UAV logistics is an important component of Urban Air Mobility (UAM), driving the prosperity and development of the urban air transportation industry [3]. Electric Vertical Takeoff and Landing UAVs (eVTOL) [4] are crucial transportation tools in the UAM field, offering unique advantages, such as low operating costs [5], low noise emissions [6], and convenient takeoff and landing [7]. Many logistics companies employ eVTOL for urban logistics services. In January 2022, Brazilian aerospace company Eve partnered with Falko [8] to develop a global operational network and ordered 200 eVTOLs to support the development of urban air mobility. During 2022, Meituan [9] conducted more than 100,000 drone deliveries in Shenzhen, covering more than a dozen communities and office buildings, serving over 20,000 residents, and completing over 75,000 orders. According to a research report by Morgan Stanley [10], the eVTOL industry is projected to reach a market size of USD 300 billion by 2030. Due to the rapid development of the eVTOL industry, the density of aircraft in the urban low-altitude airspace will gradually increase. Therefore, establishing an effective urban low-altitude public route network and implementing strict aircraft access rules [11] are key challenges to ensure the safety and efficient operation of future urban air mobility systems.

Urban logistics drone transportation planning is commonly regarded as a multi-objective optimization problem, necessitating the simultaneous consideration of various interrelated objectives. This issue can be resolved through the utilization of optimization algorithms. Maiyue Chen [12] proposed the Self-Adaptive Fast Fireworks Algorithm to address large-scale optimization problems. By incorporating expressive fast explosion and inter-fireworks competitive cooperation mechanisms, the algorithm enriched the search space and achieved adaptive tuning of the hyperparameters. This approach demonstrated improved solving capabilities and faster convergence speed. In Junayed Paha's [13] investigation of vehicle routing problems with a factory-in-a-box, a multi-objective hybrid metaheuristic algorithm was devised with the objective of minimizing the costs associated with early arrivals, delays, and compensations. This algorithm yielded optimal delivery routes for warehouses, suppliers, and customers. For the allocation and scheduling issue concerning ship berths, Maxim A. Dulebenets [14] developed the Diffusion Memetic Optimizer (DMO). Through interactive evolution during the DMO process, the optimizer promoted diffusion within the network search space, facilitating the identification of the optimal solution.

Currently, there have been preliminary explorations of urban low-altitude route network research both domestically and internationally. NASA [15] has established a radial intercity air traffic route network centered around the Dallas Vertical Takeoff and Landing Port, connecting 19 surrounding cities' vertical takeoff and landing airports. By implementing aircraft safety intervals and departure time intervals, they have successfully achieved aircraft scheduling and sequencing at the vertical airports. Nanyang Technological University [16] has proposed the concept of managing urban airspace in an adaptive manner, discussing three types of urban low-altitude air route networks: the AirMatrix network, the over-buildings network, and the over-roads network. With the optimization objective of minimizing the distances, the concepts of non-intersecting channels, and the first-come-first-served principle, they have developed a routing algorithm to determine the optimal routes under different network configurations. Chan, Y.Y., et al. [17] proposed an energy-efficient path-planning model for unmanned aerial vehicles in a large-scale and complex urban environment considering wind dynamics. Firstly, the complex urban environment was decomposed into a network model using Voronoi diagrams, which enabled the acquisition of feasible initial paths. Then, by taking into account the non-linear energy consumption along the paths, the Particle Swarm Optimization (PSO) metaheuristic algorithm was employed to obtain ultimately an optimal path characterized by a short distance, low energy consumption, and the avoidance of collisions. Based on the spatial distribution characteristics of takeoff and landing points, Hao Peng [18] established a horizontal main route network without obstacle constraints using the Voronoi diagram. They also determined the altitude levels for each segment and proposed a branch route design based on an improved ACO-Dubins algorithm, further reducing the risk of conflicts during aircraft takeoff and landing processes. Bizhao Peng et al. [19] divided the urban airspace into an AirMatrix ConOps traffic network model. Based on the route network and risk cost matrix, they utilized the A* cost algorithm to search for cost-effective paths for UAVs. However, this algorithm was superior to the Dijkstra algorithm only in terms of computation time and was not as effective as the Dijkstra algorithm in reducing the total risk costs. Li Shan et al. [20], considering the complex urban low-altitude environment and the constraints of the UAV's performance, proposed a route network planning method based on improved cellular automata and minimum spanning tree algorithms to construct an aerial route network by selecting the optimal routes. In summary, there are currently two types of urban low-altitude route network planning methods: on-demand allocated central radiation networks [21] and route networks relying on urban infrastructure [22]. Although these methods are effective for small-scale UAVs transportation, their efficiency significantly decreases as the scale of the UAVs increases. This can lead to excessive route network density and wastage of the airspace resources.

To address the existing design issues of urban low-altitude route networks, this study considers urban airspace constraints and the UAV's performance and proposes a public route-network-planning method based on Voronoi diagrams and the A* algorithm. The initial route network utilizing the Voronoi diagram is established. One of its advantages lies in its ability to allocate flight paths effectively while ensuring comprehensive coverage of the urban airspace. By employing the A* algorithm for obstacle avoidance in path planning, it is possible to search efficiently for the shortest routes, thereby reducing time and resource consumption. The specific steps of the planning method are as follows: Firstly, construct a city airspace grid model in which the characteristics of the airspace are mapped onto the grid map. Introduce an obstacle clustering algorithm based on DBSCAN to generate representative obstacle points as the Voronoi seed nodes. Utilize the Voronoi diagram to establish the initial route network. Then, conduct an improved path planning by employing the A* algorithm for obstacle avoidance in route edges that pass through obstacles. To ensure the safe operation of the drones, set constraints on the route safety interval. This process will generate a low-altitude public air route network for urban areas. After considering the cost of logistics drone flights at different heights, determine the layout heights of the route network. Finally, establish multiple metrics to evaluate the rationality and applicability of the network.

2. Problem Description and Modeling

2.1. Problem Description and Model Assumptions

The problem investigated in the study presented in this paper is the construction of a low-altitude UAV public route network for urban logistics. As the terminal distribution network for UAVs has not yet been established, the large-scale free operation of drones cannot meet the safety and efficiency requirements of urban airspace traffic, which is detrimental to the security management of the UAV system network. Therefore, the purpose of this study is to establish a UAV public route network in the low-altitude urban airspace, enabling the UAV to avoid obstacles during a low-altitude flight while making full use of the urban airspace resources. To ensure the safe operation of the UAV and reduce the complexity of network management, a unified high-altitude terminal distribution route network is constructed in this study.

The model assumptions are as follows:

(1) The location of the supply center and each logistics demand point is known.

(2) The UAV can perform only ascent or descent operations in takeoff and landing areas, and horizontal flight is the only option in other areas.

(3) The UAV maintains a constant flight speed during flight.

2.2. Urban Airspace Environment Modeling

A combination of the Digital Elevation Model (DEM) and the grid method is used to model the urban airspace environment. The urban spatial region is denoted as D, and the function expression of DEM in the region is given as $V_p = (x_i, y_i, z_i)$, where $(x_i, y_i) \in D$ represents the plane coordinate and z_i represents the elevation corresponding to (x_i, y_i). The space D is divided into u×v grids, and the grid center is denoted by p_{mn}. The unit grid accuracy is l_g, m and n represent the serial numbers of the grid center in the x and y directions of the space D, $m = 1, 2, \ldots u$ and $n = 1, 2, \ldots v$. The coordinates of p_{mn} are $p(x_i, y_i)$, where $x_i = m \times l_g$ and $y_i = n \times l_g$.

This paper considers urban airspace obstacles as high-rise buildings, no-fly zones, and signal interference zones. A modeling diagram is shown in Figure 1. The blue region corresponds to high-rise buildings, while the red section indicates the designated no-fly zone. The yellow area denotes regions susceptible to signal interference. These obstacle areas are gridded and mapped to the grid map, The grid risk values for urban airspace allocation with different characteristics are shown in Table 1; grid cells assigned a value of 1 are excluded from expansion as path points, while the remaining grid cells are eligible for expansion.

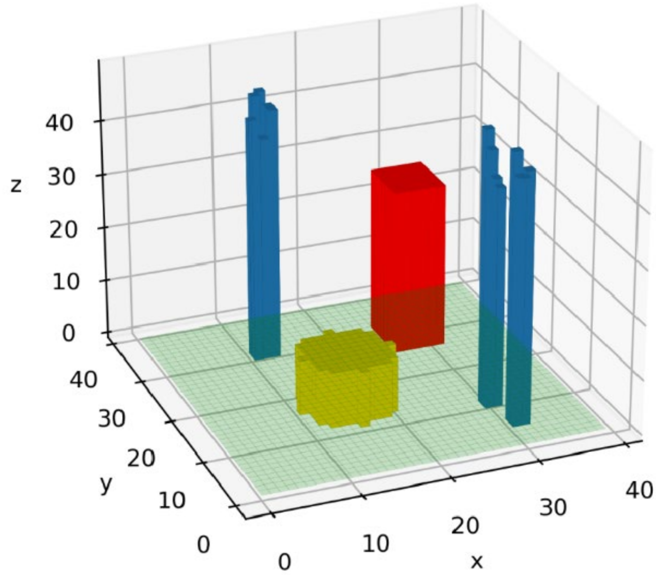

Figure 1. Schematic diagram of modeling.

Table 1. Grid risk value.

City Airspace Category	Grid Risk Value
High-rise buildings	1
No-fly zones	1
Signal interference zones	1
Free airspace	0

3. Method for Public Air Route Network Planning

3.1. Obstacle Clustering Based on DBSCAN

The Voronoi diagram is used to divide the Voronoi cells based on seed nodes [23]. The more nodes used for graph searching, the higher the computational time and space complexity. Therefore, before route planning, a representative obstacle point set must be generated as the Voronoi seed nodes to improve the efficiency of the graph searching.

DBSCAN is a density-based spatial clustering algorithm that does not require the number of clusters to be determined in advance and can effectively discover clusters of different shapes. Given a data set $O = \{x_1, x_2 \ldots, x_n\}$, there are two important parameters, R_{esp} and $MinPts$, which describe the density of the sample data distribution in the neighborhood. R_{esp} describes the neighborhood distance threshold (radius) of a sample point, and $MinPts$ describes the minimum number of samples in the neighborhood with a radius of R_{esp}. Let the x_i neighborhood set of R_{esp} be denoted as

$$N(x_i) = \{x_j | dist(x_i, x_j) \leq R_{esp}\} \quad (1)$$

where $dist(x_i, x_j)$ represents the distance between two points and R_{esp} is the neighborhood radius. If x_i is a core point, it needs to satisfy

$$|N(x_i)| \geq MinPts \quad (2)$$

where $|N(x_i)|$ is the number of samples in the x_i neighborhood and $MinPts$ is the density threshold. The DBSCAN clustering process is as follows:

Step 1: Input all points in the data set O;

Step 2: Determine the values of R_{esp} and $MinPts$;

Step 3: Define the Euclidean distance between two sample points;

Step 4: Traverse the R_{esp} of each point in the data set. If $|N(x_i)| \geq MinPts$, mark x_i as a core point and create a cluster with that point as the core;

Step 5: Iteratively cluster all objects with a density reachable from the core points and add them to the corresponding clusters;

Step 6: When no new points are added to any clusters, the algorithm ends.

Figure 2 is a schematic diagram of the obstacle clustering based on DBSCAN. The black area represents obstacles, the yellow dots represent gridded obstacle nodes, and the red pentagrams represent the Voronoi seed nodes.

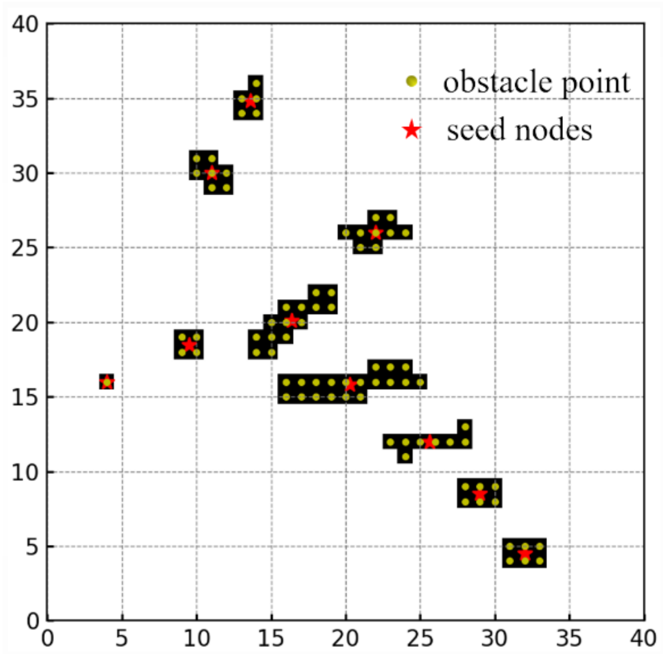

Figure 2. Obstacle clustering.

3.2. Public Air Route Network Modeling

3.2.1. Construction of the Initial Public Air Route Network

The most prominent advantage of the Voronoi diagram in path-planning problems is that the calculated path can be far away from obstacles [24]. A Voronoi seed node set is obtained by obstacle clustering, as in Section 3.1, denoted as $P = \{p_1, p_2 \ldots, p_n\}$, $(i = 1, 2, \ldots n)$, where p_i is any point in the set. The Voronoi region corresponding to p_i is defined as

$$V(p_i) = \{p|dist(p, p_i) < dist(p, p_j), p_i \neq p_j, p \in P\} \tag{3}$$

where $V(p_i)$ is called the Voronoi region of point p_i and $dist(p, p_i)$ represents the Euclidean distance between points p and p_i. Figure 3 shows the Voronoi diagram generated based on the obstacle information, including route nodes and route edges. The initial route network generated from the Voronoi diagram is defined as $G(V, E)$, V is the set of route nodes, and E is the set of route edges.

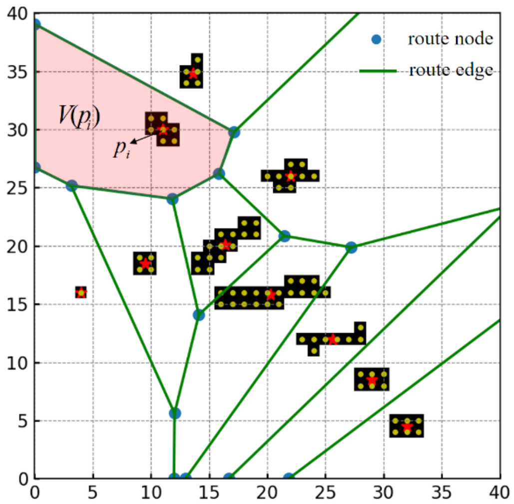

Figure 3. An example of a Voronoi diagram based on obstacles.

3.2.2. Method of Public Air Route Network Improvement Planning

Due to the presence of obstacles of varying shapes and sizes, the Voronoi diagram may generate unreachable nodes and edges. Therefore, an improved planning of the initial Voronoi diagram is required, which includes two steps. The first step involves deleting the route nodes located inside the obstacles. The second step involves using the A* algorithm for obstacle-avoidance planning for the route edges that pass through obstacles. The algorithm is described as follows:

A* algorithm is a heuristic path-planning algorithm suitable for solving path trajectories with known global obstacle information, and its search direction is set to eight directions. The A* algorithm is represented by the evaluation function $f(n)$:

$$f(n) = g(n) + h(n) \tag{4}$$

where n is the current point, $g(n)$ is the actual cost function from the starting point to the current point, and $h(n)$ is the heuristic function which represents the estimated cost from the current node to the end point.

(1) Actual cost function

Assume the starting point coordinates are (x_0, y_0), the ending point coordinates are (x_e, y_e), and the coordinates of the intermediate point on the path are (x_n, y_n). The actual cost of the drone from the starting point to the intermediate point is defined as:

$$g(n) = \sum_{i=1}^{n} \sqrt{(x_i - x_{i-1})^2 + (y_i - y_{i-1})^2} \tag{5}$$

(2) Heuristic function

Due to the existence of dense obstacles in urban environments, using the Euclidean distance as the heuristic function will produce a distance that is significantly smaller than the actual flight distance, while those obatined from using the Manhattan distance will be significantly larger than the actual flight distance. Therefore, this study uses a linear combination of the Euclidean distance and Manhattan distance as the heuristic function, expressed as

$$h(x) = \sqrt{(x_e - x_n)^2 + (y_e - y_n)^2} + (|x_e - x_n| + |y_e - y_n|) \tag{6}$$

(3) Path simplification

Due to the limitation of search directions, there may be unnecessary turning points in the optimal path [25], as shown in Figure 4. It can be seen that the line from point O to point B does not pass through obstacles. Therefore, the redundant node A between point

O and point B can be removed, and O and B can be directly connected. Next, connect each node and determine whether the connection passes through obstacles. If it does not pass through, delete the redundant nodes between the connections. Finally, the simplified optimal path O-B-C-D is obtained.

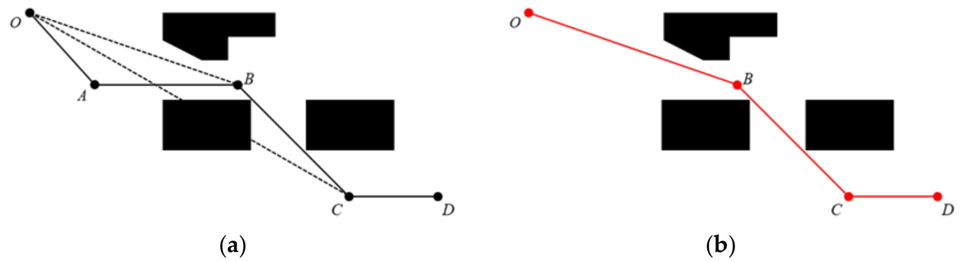

Figure 4. Path simplification process: (**a**) represents the path before simplifying and (**b**) represents the path after simplifying.

The A* algorithm route-improvement planning steps are shown in Figure 5:

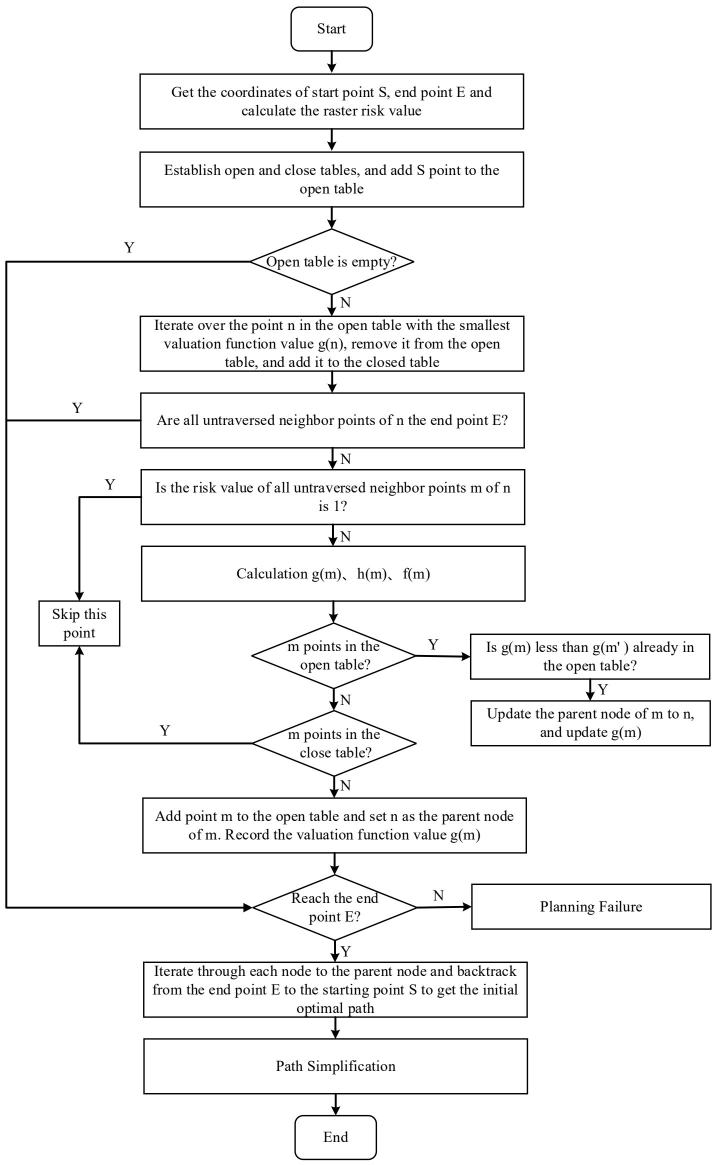

Figure 5. Flow of algorithm.

3.3. Establishment of Route Safety Separation Constraints

After the construction of the public air route network, there may be dangerous situations where some route edges and the improved A* segments are too close to obstacles, which cannot guarantee a safe obstacle-avoidance flight. Therefore, constraint conditions for route safety separation are established, and the safety separation between the logistics drone and the obstacle is defined as

$$w_{s,i} = r_{\min,i} - \frac{l_g}{2} \geq D_{min} \tag{7}$$

where $w_{s,i}$ is the safety separation of the i segment, $r_{\min,i}$ is the shortest distance from the obstacle to the segment i, l_g is the grid accuracy, and D_{min} is the minimum safety separation. By establishing the safety separation constraint, the danger level of the segment i can be represented by the risk level $w_{d,i}$:

$$w_{d,i} = \begin{cases} 1 \quad w_{s,i} < D_{\min} \\ \frac{D_{\max} - w_{s,i}}{D_{\max} - D_{\min}} \; D_{\min} \leq w_{s,i} \leq D_{\max} \\ 0 \quad w_{s,i} > D_{\max} \end{cases} \tag{8}$$

where D_{max} is the maximum safety separation.

3.4. Determination of the Best Flight Altitude

The optimal flight altitude of a drone is determined by minimizing the horizontal and vertical flight costs, balancing the horizontal path cost saved by cruising at a higher altitude and the additional cost added during the vertical process. This study assumes that all drones take off and land from the ground. According to reference [26], the shortest horizontal path is generated by the A* algorithm at each candidate altitude layer, and the total cost of each altitude layer, which includes the horizontal flight cost and the vertical flight cost, is calculated. Assuming that the flight cost is proportional to the flight distance, the unit cost ratio between the horizontal and vertical flights is $p_h : p_v$. Then, the optimal flight altitude corresponding to the lowest total flight cost is determined as the best flight altitude.

3.5. Evaluation Indicators of the Public Air Route Network

3.5.1. Path Evaluation Indicators

(1) Energy Cost

The energy cost of the UAV is proportional to the length of the path:

$$J_{energy} = \sum_{i=1}^{n} \mu \times l_i \tag{9}$$

where J_{enerey} is the path energy cost, μ is energy cost scaling factor, and l_i is the segment length.

(2) Risk Cost

Take the risk level $w_{d,i}$ of the segment as the risk cost of the path:

$$J_{risk} = \sum_{i=1}^{n} \beta \times w_{d,i} \tag{10}$$

where J_{risk} is the path risk cost and β is risk factor.

(3) Total Path Cost

The total cost of the path is expressed as the sum of the energy cost and the risk cost:

$$J = \alpha_1 \times J_{energy} + \alpha_2 \times J_{risk} \tag{11}$$

where J is the total path cost, α_1 and α_2 are weight coefficients, and $\alpha_1 + \alpha_2 = 1$.

(4) Non-linear coefficient

The ratio of the route distance between two points to their straight line distance:

$$\eta = \frac{\sum_{i=1}^{n}\sum_{j=1}^{n} l_{ij}}{\sum_{i=1}^{n}\sum_{j=1}^{n} s_{ij}} \tag{12}$$

where η is non-linear coefficient, l_{ij} means the actual length of the segment between nodes i and j, and s_{ij} means the straight-line distance between nodes i and j.

3.5.2. Public Air Route Network Evaluation Indicators

(1) Total Length of Network

To avoid dangerous areas, such as high-rise buildings, no-fly zones, and signal interference zones, the route network is constructed to avoid obstacles, and the total length of the public air route network is the sum of all route edge lengths:

$$TL = \sum_{i=1}^{M} l_i \tag{13}$$

where TL is the total length of network and M is the number of edges.

(2) Average Degree

The degree k_j of node j in the network is the number of routes directly connected to the node. The average degree of the network is the average value of the degrees of all nodes in the network:

$$\begin{aligned} k_j &= \sum_{j=1}^{m} a_{ij} \\ \langle k \rangle &= \frac{1}{m}\sum_{j=1}^{m} k_j \end{aligned} \tag{14}$$

where m is the number of nodes; if nodes i and j are connected, a_{ij}= 1, otherwise, a_{ij}= 0; and $\langle k \rangle$ is the average degree.

(3) Maximum Route at Intersection

In the route network, the maximum route at intersection represents the maximum value of the degree of the node, that is

$$C = max\{k_1, k_2 \ldots, k_m\} \tag{15}$$

where C is the maximum route at intersection.

(4) Reachability of Route Network

The ease of a drone to reach a certain location is represented by the average flight time, that is:

$$\begin{aligned} \langle t \rangle &= \frac{L}{v} \\ L &= \frac{2}{m(m-1)}\sum_{i \neq j} d_{ij} \end{aligned} \tag{16}$$

where $\langle t \rangle$ is the average flight time, L is the average shortest path length in the network, v is the drone's flight speed, and d_{ij} represents the shortest distance between nodes i and j.

(5) Airspace Coverage

$$AC = \frac{rc}{tc} \tag{17}$$

where AC is airspace coverage, rc is the actual coverage area, and tc is the total airspace area.

4. Shortest-Path Search Method for Public Air Route Network

Dijkstra's algorithm is a typical single-source shortest-path algorithm, used to calculate the shortest path from a node to all other nodes. The supply and demand points are added to the route network, and the shortest path between each pair of OD is searched using the Dijkstra algorithm. Since the obtained initial shortest path has corners and does not meet the requirements of a drone flight, it needs to be smoothed. In this study, B-splines are used to optimize the obtained initial shortest path.

5. Simulation Analysis

5.1. Simulation Environment

In this study, the regional geographic information altitude data of Shanghai are used for simulation. The selected area is a square matrix of 4 km $\times$ 4 km, as shown in Figure 6. A 200 $\times$ 200 matrix is obtained by gridding the urban airspace environment. In accordance with the Provisional Regulations on Flight Management of Unmanned Aerial Vehicles (Draft) approved by the State Council [27] issued by the Central People's Government of the People's Republic of China and the relevant data collection and analysis, the simulation parameters and UAV performance parameters are selected, as shown in Table 2 [20,26,28].

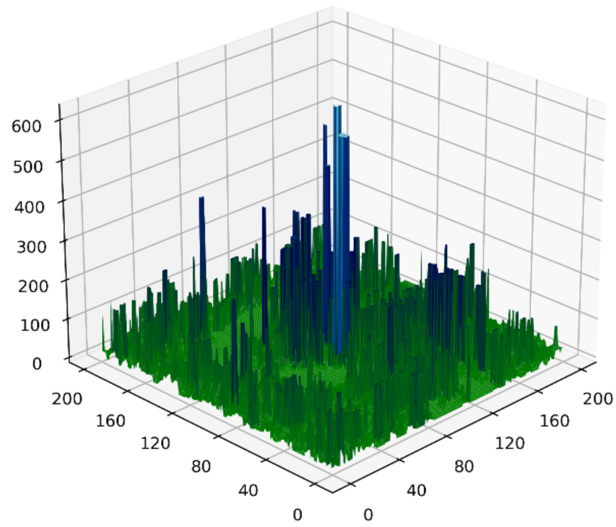

Figure 6. Simulation environment.

Table 2. Simulation parameter settings.

Parameter	Value	Parameter	Value
Maximum range of UAV, km	20	Maximum flight height of UAV, m	200
Maximum turning angle of UAV, °	$\pi/2$	Vertical flight unit cost p_v	3.2
Grid accuracy, l_g/m	20	Horizontal flight unit cost p_h	1
Minimum safety separation, D_{min}/m	10	UAV speed, $v/(\mathrm{m \cdot s^{-1}})$	12
Energy cost scaling factor μ	0.5	Risk factor β	10
Energy cost weight α_1	0.6	Risk cost weight α_2	0.4

5.2. Optimal Flight Altitude

During the process of determining the optimal flight altitude, an A* algorithm is employed to generate the horizontally shortest obstacle-free path for each candidate altitude layer. Figure 7 illustrates a set of examples depicting the shortest paths generated for candidate altitudes of 30 m, 70 m, 110 m, and 150 m, respectively. The dot is the origin point, the star is the destination point, and the yellow line segment is the shortest path. As the candidate altitude increases, the length of the flight path decreases. This indicates that longer horizontal paths are needed to avoid obstacles at lower altitudes, while the horizontal path length can be shortened by raising the flight altitude. The randomly set OD pair distances range from 1 km to 4 km. Table 3 shows the average shortest horizontal path length and the average total cost for 50 sets of OD pairs at different altitudes. It can be seen that the average total flight cost is lowest at the altitude level of 110 m. When the candidate altitude is below 110 m, increasing the flight altitude can significantly reduce the horizontal flight distance due to a increased presence of obstacles. However, when the candidate altitude exceeds 110 m, the added vertical cost outweighs the saved horizontal cost. Therefore, this altitude is the best flight altitude for a given ratio of horizontal cost to vertical cost.

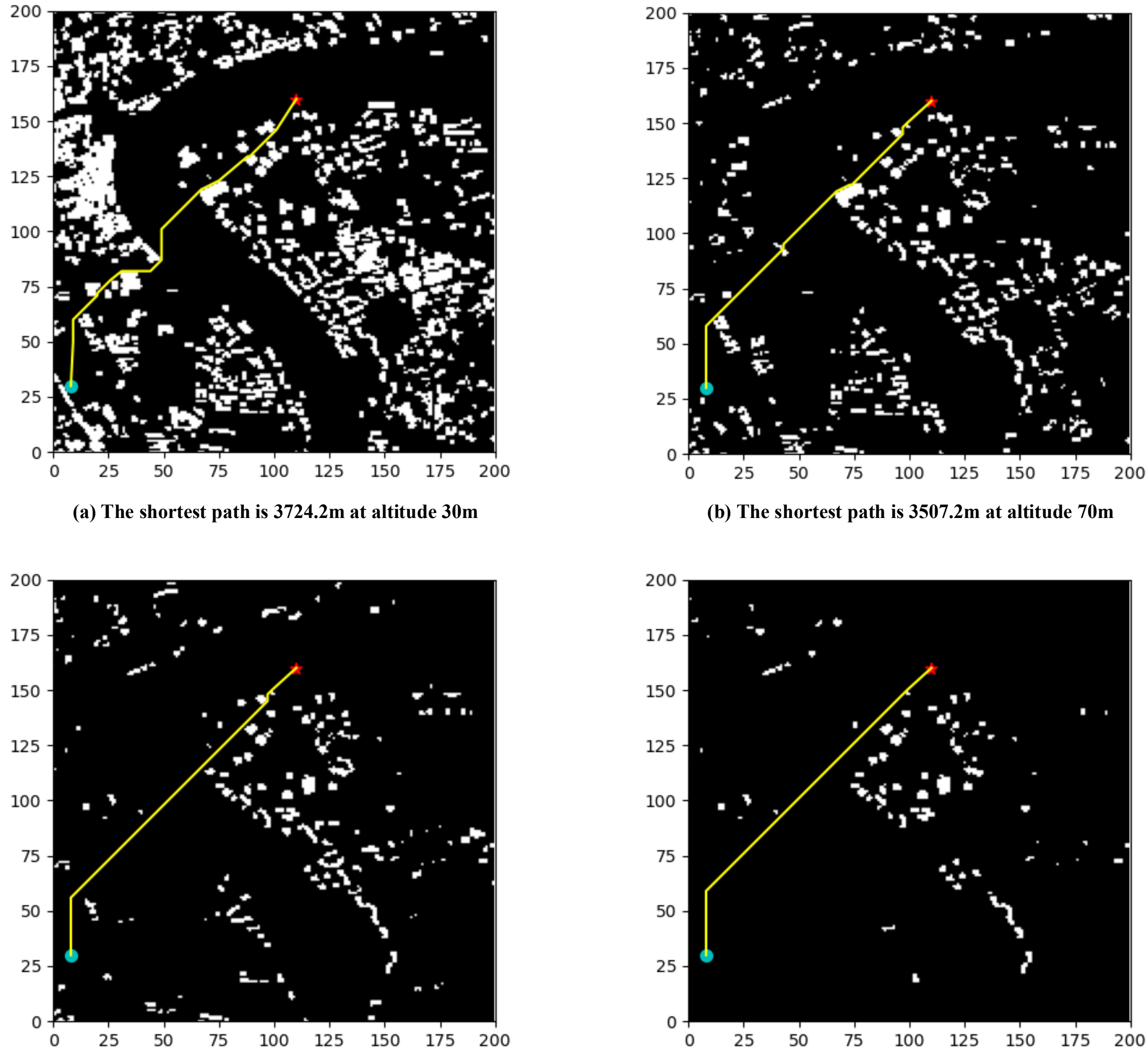

(a) The shortest path is 3724.2m at altitude 30m

(b) The shortest path is 3507.2m at altitude 70m

(c) The shortest path is 3348.2m at altitude 110m

(d) The shortest path is 3336.4m at altitude 150m

Figure 7. Shortest path with different candidate heights.

Table 3. Average shortest path length and average total cost.

Candidate Height Level	Average Shortest Horizontal Path Length, m	Average Total Cost
30 m	2485	2581
70 m	2128	2352
110 m	1975	2327
150 m	1927	2407

5.3. Simulation Analysis of the Route Network

Based on the optimal flight altitude determined above, the constructed urban low-altitude public route network is obtained, as shown in Figure 8 below. The red line is the air route network, which is arranged at the altitude level of 110 m.

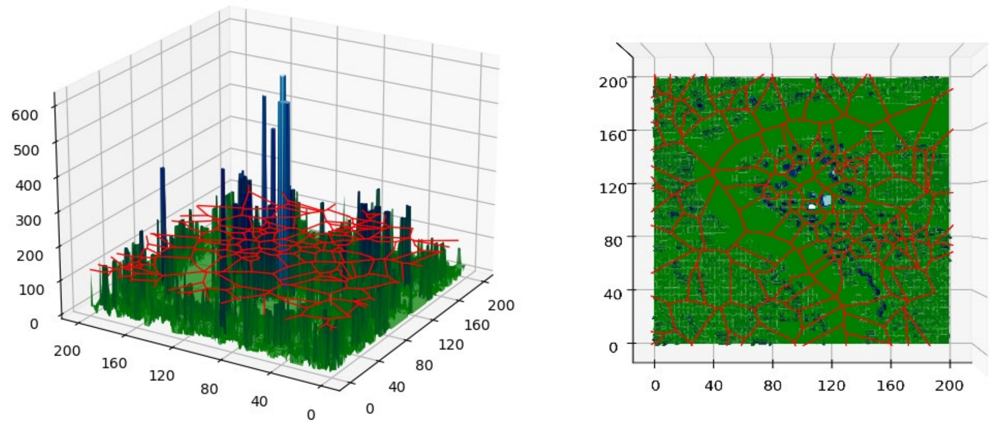

(**a**) (**b**)

Figure 8. The air route network: (**a**) represents the isometric view and (**b**) represents the top view.

To better reflect the superiority of the air route network constructed in this study, a comparison is made with the city-road-network-planning method and the central-radial-network-planning method. The city-road network has natural obstacle avoidance conditions, enabling the use of aerial delivery of the logistics drones above it to mitigate the collision risks associated with operational anomalies. The city-road network data are imported into ArcGIS for data preprocessing, and topological analysis is performed to output the road nodes and edges, resulting in the network shown in Figure 9. Based on the distribution of takeoff and landing points within the region, a central radial network is established, as shown in Figure 10.

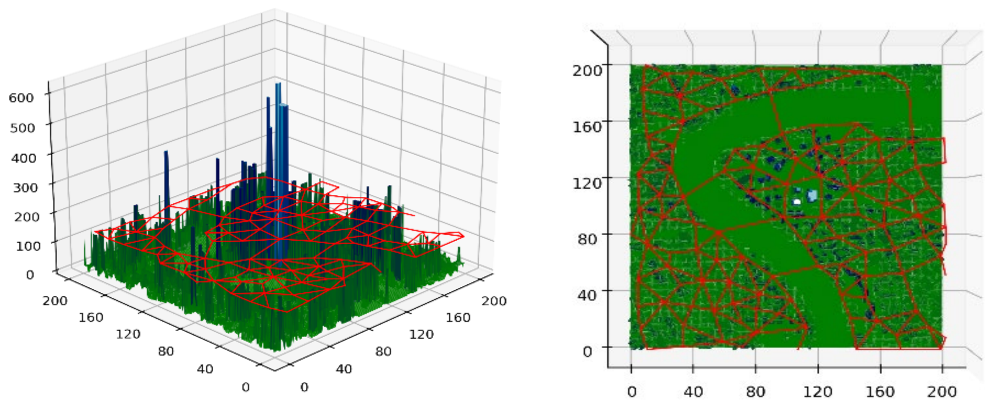

(**a**) (**b**)

Figure 9. The city road network: (**a**) represents the isometric view and (**b**) represents the top view.

The results of the three network features in the same simulation scenario are shown in the Table 4.

Table 4. Comparison table of network feature results.

Network Type	***TL*, km**	***C***	**⟨*k*⟩**	***AC*, %**	**⟨*t*⟩, s**
Air route network	84.67	3	2.51	97.12	198.5
City road network	90.71	7	3.83	87.29	217.9
Central radial network	92.27	10	7.82	62.14	202.2

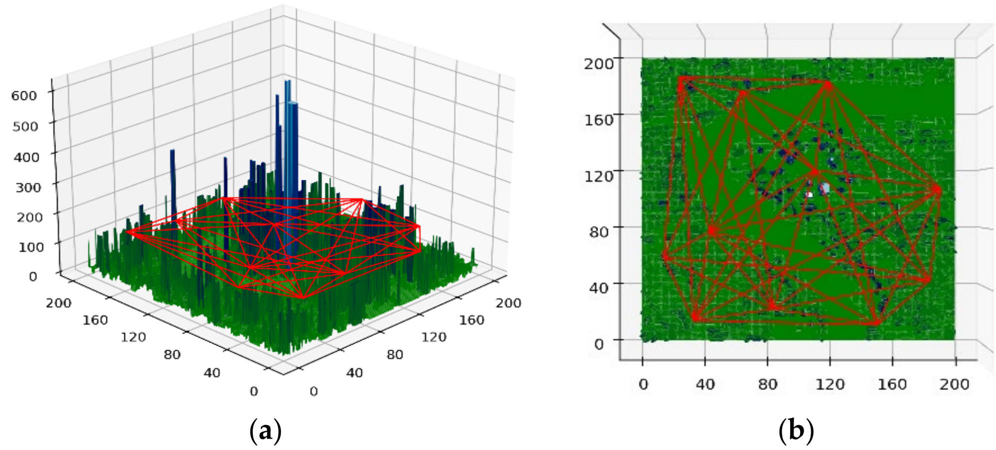

Figure 10. The central radial network: (**a**) represents the isometric view and (**b**) represents the top view.

Through comparative analysis, the air route network constructed in this study is compared with the urban-road-network-planning method—the total network length is shortened by 7.1%, the maximum number of intersection routes is reduced by 133%, the average network degree is decreased by 52.6%, the airspace coverage is increased by 9.8%, and the average flight time is reduced by 19.4s. Compared with the central-radial-network-planning method, the air route network has a 9% reduction in total length, a 233% decrease in the maximum number of intersecting routes, a 212% decrease in network average degree, a 35% increase in airspace coverage, and a decrease in average flight time by 3.7s. Therefore, the proposed method in this paper has shorter total network length, fewer intersection conflicts, higher airspace coverage, and better network reachability, which reduces the risk of route conflicts and makes the route network management less difficult.

5.4. Shortest-Path Search Simulation Analysis

To verify the effectiveness of the route network constructed in this study, a path search simulation is carried out. One supply point and ten demand points are set centrally, and the specific coordinate parameters are set, as listed in Table 5.

Table 5. Location information of supply and demand points.

Number	Type	Coordinates
1	S	(110, 120)
2	D	(25, 185)
3	D	(84, 23)
4	D	(15, 59)
5	D	(182, 43)
6	D	(189, 182)
7	D	(44, 77)
8	D	(189, 107)
9	D	(118,182)
10	D	(34, 15)
11	D	(149, 12)

To comply with the minimum safety separation requirements for drone flights while considering the uncertainties of drone operating conditions and measurement errors, the route safety separation is set to be no less than 5 m, 10 m, 15 m, 20 m, 25 m, and 30 m. The energy and risk cost of the route are calculated by the Formulas (9) and (10). According to the initial path of the air route network and the route safety interval constraints, the optimal route path is obtained, as shown in Figure 11 and Table 6. The green line is the air route network and the yellow line is the optimal path searched for. It can be observed that as the safety interval increases, the path gradually moves away from the obstacle area, resulting in an increase in the average length of a single flight path, average flight time, and detour distance, while the path risk decreases. Based on Formula (11), we calculate the total cost of the path under different safety intervals. Specifically, when the safety interval of the flight route is set to 15 m, the total path cost value is the smallest at 722.8; when the safety interval is set to 30 m, the total path cost value is largest at 762.6.

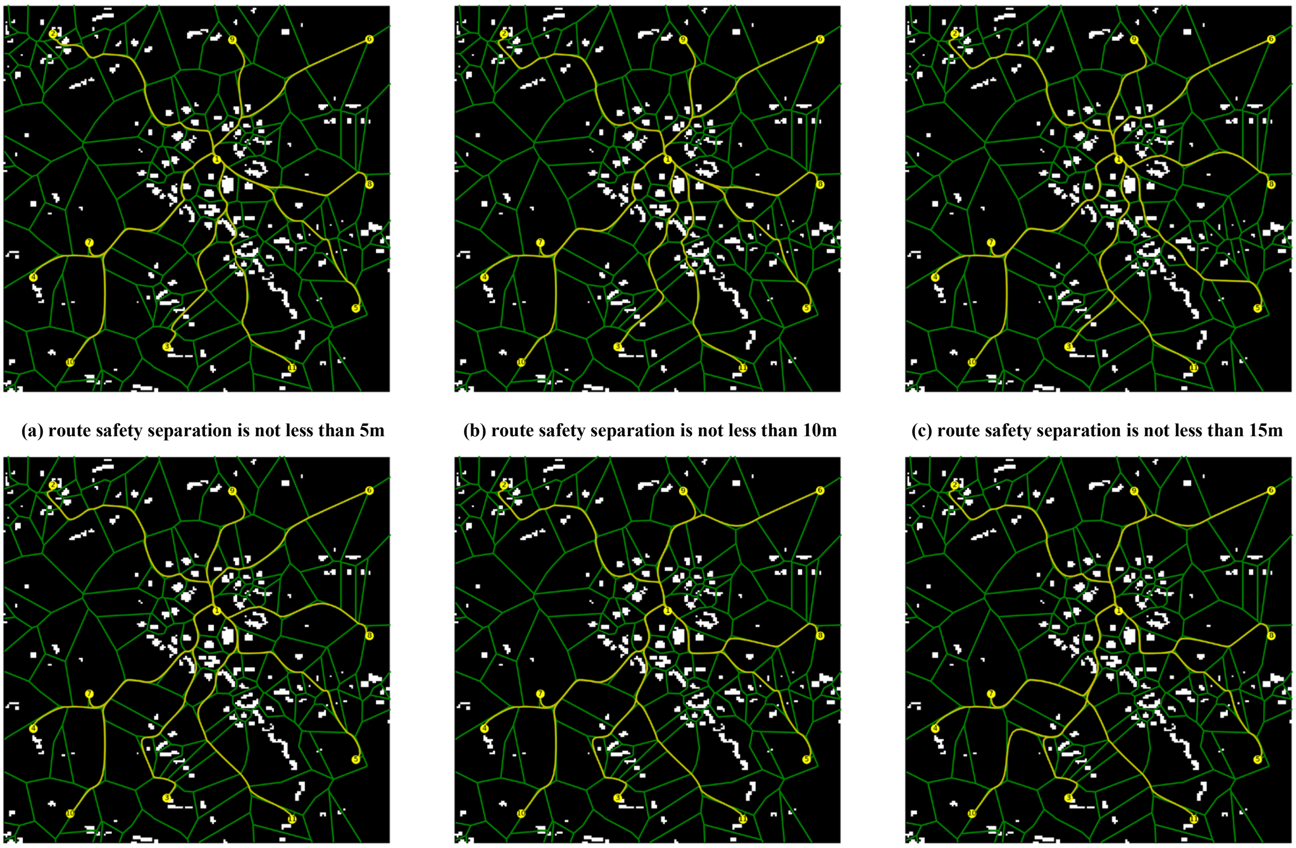

(a) route safety separation is not less than 5m (b) route safety separation is not less than 10m (c) route safety separation is not less than 15m

(d) route safety separation is not less than 20m (e) route safety separation is not less than 25m (f) route safety separation is not less than 30m

Figure 11. Optimal paths with different safety intervals.

Table 6. Optimal path feature values.

Safety Interval	Average Single Path Length, m	Averages Flight Time, s	Non-Linear Coefficient	Energy Cost	Risk Cost	Total Path Cost
5 m	2286	190.5	1.15	1143	151.28	746.3
10 m	2313	192.8	1.17	1156.5	125.2	743
15 m	2363	196.9	1.19	1181.5	34.64	722.8
20 m	2403	200.3	1.21	1201.5	13.6	726.3
25 m	2473	206.1	1.25	1236.5	3.6	743.3
30 m	2542	211.8	1.28	1271	0	762.6

Through the analysis of the simulation results, when considering both the energy cost and risk cost of the path comprehensively, we find that the total cost of the path follows a trend of initially decreasing and then increasing as the safety interval increases. This is because a larger safety interval at the beginning allows the path-planning algorithm to avoid more obstacles, providing greater flexibility in selecting the path from a wide range of available spaces, thus reducing the total cost. However, as the safety interval continues to increase, the path-planning algorithm may need to deviate from a straight-line path and choose a longer route to bypass obstacles. This leads to an increase in the overall path length and, consequently, an increase in the total cost. By balancing these two factors, selecting a balanced safety interval in path planning allows us to obtain an optimal path with the minimum total cost.

5.5. Discussion

To summarize, the urban low-altitude flight route network constructed in the study presented in this paper has the capability to allocate flight paths in a rational manner, enhance the coverage of urban airspace, reduce conflict risks at intersections, and decrease the overall network density. Furthermore, by employing the Dijkstra algorithm to solve the network model, it was possible to determine the optimal path with the minimum total cost. In future research, our focus will remain on optimizing the urban logistics drone route network. This will be accomplished through the establishment of multi-objective network planning models and the application of advanced optimization algorithms, aiming to maximize transportation efficiency, maximize profits, and minimize risks. These efforts will drive the development and application of urban air mobility.

6. Conclusions

This research paper presents a novel approach for planning a public network of low-altitude logistics UAVs in urban areas, which utilizes obstacle-based Voronoi diagrams and A* algorithms. This facilitates an efficient and comprehensive coverage of the urban area, optimizing the utilization of the available airspace resources. The Voronoi diagram effectively maximizes the utilization of the gaps between obstacles, allowing for the generation of safe flight paths that maintain a maximum distance from all obstacles. To enhance the efficiency of the Voronoi diagram generation, we employ the DBSCAN clustering algorithm to generate representative obstacle points as the Voronoi seed nodes. Furthermore, we utilize the A* algorithm for obstacle-avoidance planning for the route edges that pass through obstacles and for minimizing unnecessary turns. Additionally, we establish safety interval constraints for each route in the air route network to ensure safe operating conditions. By balancing the flight costs of logistics UAVs at different altitudes, the route network layout height is determined. Based on the research methodology proposed in this study, a city low-altitude air route network with short total routes, low conflict risk, high airspace coverage, and good network accessibility can be ultimately obtained.

Based on authentic geographical information data, the proposed methodology can provide optimal routes for UAVs and improve the overall efficiency of logistics and transportation operations in urban areas. Moreover, the reduction in conflict risks and the expansion of airspace coverage contribute to enhancing the safety and operational reliability of the air route network, thereby exerting a positive impact on the fields of logistics, transportation, and other related sectors.

In the future, we will carry out more flight mission simulation scenarios, increase the consideration of external factors, and apply the models and methods proposed in this paper to the construction of an urban low-altitude route network in real scenarios, providing strong support for the planning and management of an urban low-altitude route network and realizing an efficient, safe, and sustainable urban air mobility system.

Author Contributions: Conceptualization, H.Z.; investigation, O.F.; data curation, S.W.; writing—original draft, T.T.; supervision, G.Z. All authors have read and agreed to the published version of the manuscript.

Funding: This research was funded by the National Natural Science Foundation of China (No. 71971114) and the Fundamental Research Funds for the Central Universities (No. NQ2022012).

Institutional Review Board Statement: Not applicable.

Informed Consent Statement: Not applicable.

Data Availability Statement: Not applicable.

Acknowledgments: The authors acknowledge with thanks the support for this work by the College of Civil Aviation at Nanjing University of Aeronautics and Astronautics.

Conflicts of Interest: The authors declare no conflict of interest.

References

1. Byung, D.S.; Kyungsun, P.; Kim, J.H. Persistent UAV Delivery Logistics: MILP Formulation and Efficient Heuristic. *Comput. Ind. Eng.* **2018**, *120*, 418–428.
2. Zhang, H.H.; Zhang, L.D.; Liu, H.; Zhong, G. Track Planning Model for Logistics Unmanned Aerial Vehicle in Urban Low-altitude Airspace. *J. Transp. Syst. Eng. Inf. Technol.* **2022**, *22*, 256–264.
3. Li, C.L.; Qu, W.Q.; Li, Y.D.; Huang, L.Y.; Wei, P. Overview on traffic management of urban air mobility (UAM) with eVTOL aircraft. *J. Trfc. Trnsp. Eng* **2020**, *20*, 35–54.
4. Quan, Q.; Li, G.; Bai, Y.Q. Low altitude UAV traffic management: An introductory overview and proposal. *Acta Aeronaut. Astronaut. Sin.* **2020**, *41*, 6–34.
5. Dukkanci, O.; Kara, B.Y.; Bektas, T. Minimizing energy and cost in range-limited drone deliveries with speed optimization. *Transp. Res. Part C* **2021**, *125*, 102985. [CrossRef]
6. Smith, A.; Dickinson, J.E.; Marsden, G.; Cherrett, T.; Oakey, A.; Grote, M. Public acceptance of the use of drones for logistics: The state of play and moving towards more informed debate. *Technol. Soc.* **2022**, *68*, 101883. [CrossRef]
7. Mazur, A.M. Regulatory framework on the UAM operational concepts of the ASSURED-UAM project. *Aircr. Eng. Aerosp. Technol.* **2022**, *94*, 1491–1498. [CrossRef]
8. China Aviation News. Eve and Falko Announce Collaboration to Develop Global Operations Network. Available online: https://www.cannews.com.cn/2022/0113/337597.shtml (accessed on 13 January 2022).
9. Liu, X.P. Meituan Drone Assists in the “Last Three Kilometers” Delivery. *China Logist. Purch.* **2022**, *655*, 28–29.
10. China Aviation News. The Development of eVTOL Has a Long Way to Go. Available online: www.cannews.com.cn/2022/0419/342116.shtml (accessed on 19 April 2022).
11. Liao, X.H.; Qu, W.Q.; Xu, C.C. A review of urban air mobility and its new infrastructure low-altitude public routes. *Acta Aeronaut. Astronaut. Sin.* **2023**, *40*. [CrossRef]
12. Chen, M.Y.; Tan, Y. A Self-Adaptive Fast Fireworks Algorithm for effective large-scale optimization. *Swarm Evol. Comput.* **2023**, *80*, 101314. [CrossRef]
13. Junayed, P.; Arriana, L.N. Exact and metaheuristic algorithms for the vehicle routing problem with a factory-in-a-box in multi-objective settings. *Adv. Eng. Inform.* **2022**, *52*, 101623.
14. Maxim, A.D. A Diffused Memetic Optimizer for reactive berth allocation and scheduling at marine container terminals in response to disruptions. *Swarm Evol. Comput.* **2023**, *80*, 101334.
15. Bosson, C.; Lauderdale, T.A. Simulation evaluations of an autonomous urban air mobility network management and separation service. In Proceedings of the AIAA 2018-3365. 2018 Aviation Technology, Integration, and Operations Conference, Atlanta, GA, USA, 25–29 June 2018.
16. Mohammed, F.B.; Chi, W.C.; Wang, Z.; Huang, S.; Tan, D.Y.; Huang, T.; Low, K.H. Preliminary Concept of Adaptive Urban Airspace Management for Unmanned Aircraft Operations. In Proceedings of the AIAA Information Systems—AIAA Infotech at Aerospace, Kissimmee, FL, USA, 8–12 January 2018.
17. Chan, Y.Y.; Ng, K.K.H.; Lee, C.K.M.; Li, T.H.; Keung, K.L. Wind dynamic and energy-efficiency path planning for unmanned aerial vehicles in the lower-level airspace and urban air mobility context. *Sustain. Energy Technol. Assess.* **2023**, *57*, 103202. [CrossRef]
18. Hao, P. Obstacle Avoidance Path Planning of eVTOL Aircraft for UAM System Algorithm Research. Master’s Thesis, Xihua University, Chengdu, China, 2022.
19. Pang, B.Z.; Tan, Q.Y.; Ra, T. A Risk-based UAS Traffic Network Model for Adaptive Urban Airspace Management. In Proceedings of the AIAA AVIATION 2020 Forum, Virtual Event, 15–19 June 2020. [CrossRef]
20. Li, S.; Zhang, H.; Li, Z.; Liu, H. An Air Route Network Planning Model of Logistics UAV Terminal Distribution in Urban Low Altitude Airspace. *Sustainability* **2021**, *13*, 13079. [CrossRef]
21. Wu, Z.Q.; Zhang, Y. Integrated Network Design and Demand Forecast for On-Demand Urban Air Mobility. *Engineering* **2021**, *7*, 135–166. [CrossRef]
22. Xu, C.C.; Ye, H.P.; Yue, H.Y. lterative construction of UAV low-altitude air route network in an urbanizedregion: Theoretical system and technical roadmap. *Acta Geogr. Sin.* **2020**, *75*, 917–930.
23. Xiong, P.W.; Zhou, X.Y.; Xiong, H.J.; Zhang, T.T. Voronoi diagram generation algorithm and application for large-scaleinteractive data space partition. *J. Natl. Univ. Def. Technol.* **2022**, *44*, 129–136.
24. Li, Y.; Liu, M. Path Planning of Electric VTOL UAV Considering Minimum Energy Consumption in Urban Areas. *Sustainability* **2022**, *14*, 13421. [CrossRef]
25. Zhang, H.; Wang, F.; Feng, D.; Du, S.; Zhong, G.; Deng, C.; Zhou, J. A Logistics UAV Parcel-Receiving Station and Public Air-Route Planning Method Based on Bi-Layer Optimization. *Appl. Sci.* **2023**, *13*, 1842. [CrossRef]
26. Li, A.; Mark, H.; Zou, B. Traffic management and resource allocation for UAV-based parcel delivery in low-altitude urban space. *Transp. Res. Part C Emerg. Technol.* **2022**, *143*, 103808. [CrossRef]

27. The Central People's Government of the People's Republic of China, Provisional Regulations on the Flight Management of Unmanned Aerial Vehicles (Draft). Available online: https://www.sohu.com/a/665640349_114760 (accessed on 7 April 2023).
28. Xu, L.; Song, W.Q.; Yan, C. Tactical flight trajectory planning methods based on threat assessments and improved Voronoi graphics. *Aeronaut. Sci. Technol.* **2019**, *30*, 35–43.